

Open Access Article

**DEVELOPMENT OF A MICROELECTRONIC CONVERTER FOR RAILWAY
AUTOMATION AND TELEMCHANICAL SYSTEMS**

Nazirjon Aripov

[0000-0002-6209-5063]

Zafar Mirzarakhmedov

[0000-0002-0102-1829]

Bobomurod Rahmonov

[0000-0002-3666-6600]

Qamara Kosimova

[0000-0002-9694-1280]

Tashkent State Transport University, 1 Temiryulchilar Str., Tashkent 100069, Uzbekistan
Zafar3086@mail.ru

Abstract. The article presents proposals for the development of microprocessor transmitters to replace TSH-65 and TSH-2000, which is designed to transmit codes generated by the KPTSH transmitter to road traffic lights and locomotive traffic lights in rail circuits equipped with a four-digit microprocessor auto-lock and the CLUB system in the joint-stock company "Uzbekiston Temir Yollari".

Nowadays, microprocessor and microelectronic systems and devices are widely used in railway automation and remote control systems. The use of systems and devices for railway automation and remote control, developed on the basis of microelectronics and microprocessor elements, ensures reliable operation in comparison with systems based on electromagnetic relays.

A functional diagram of a new developed integrated microprocessor code transmitter for transmitting codes generated in railway automation and telemechanics systems has been developed. Dimmed microelectronic code of the transmitting device, work as relays TSH-65 and TSH-2000, and they are modeled in the Proteus program.

Keywords: code transmitter, microelectronic device, software, relay, contact, unit, microprocessor.

Introduction. The contacts of the road transmitter relays are quickly worn out due to dynamic continuous operation. In order to keep the level of operational reliability of auto-locking and automatic locomotive signaling devices at a high level, preventive inspection and repair of contact transmitters is carried out annually, including lubrication of friction parts, and worn contacts are replaced with new ones.

Modern code transmitters manufactured in foreign countries are facing problems of purchasing and bringing them for use in automation and telemechanics devices owned by "Uzbekistan Temir Yollari

Received: June, 13, 2022 / Revised: July ,21, 2022 / Accepted: 19, July, 2022 / Published: 13, August, 2022

About the authors : Nazirjon Aripov

Email:

" Joint Stock Company [1-15]. The solution to these problems is the production of integrated microelectronic code transmitters (IMCT).

Research Methods

Development of a functional diagram of a microelectronic code transmitter

The microelectronic code transmitter has the following advantages [16]:

- the possibility of self-control of these devices in case of errors during operation;
- small dimensions of the microelectronic pendulum device;
- no problem of contact erosion due to the use of non-contact elements;
- duration and ease of maintenance period;
- low cost;
- energy efficiency;

The functional diagram of the IMCT device is shown in fig. 1. Functional diagram of the IMCT. It consists of blocks : secure data entry module – SDEM, comparison block- CB, microcontroller 1,2- MC- 1 and MC- 2 , decoder- DC [18].

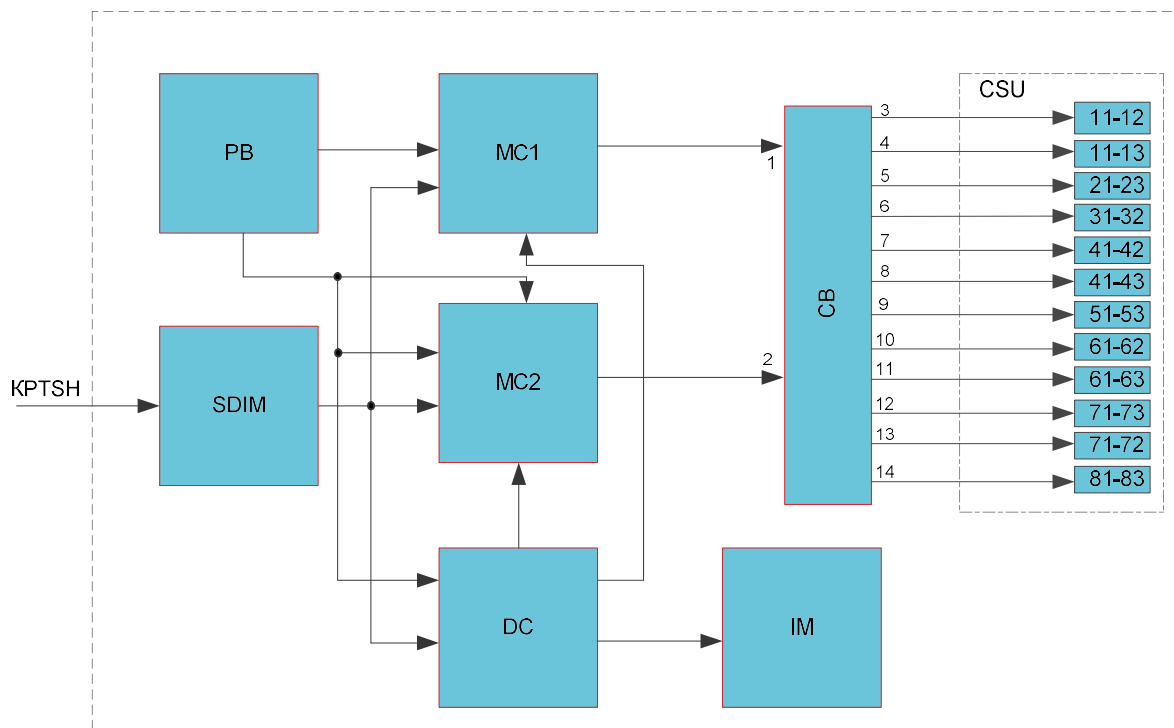


Figure 1. Functional diagram of a microelectronic code transmitter for a road transmitter.

Research Results. SDIM - a secure data input module is required for the secure connection of the microcontroller with the KPTSH. PB- the power supply unit serves to provide the microcontroller with the necessary voltage . MC1 - the 1st microcontroller, MC2 - the 2nd microcontroller MC1 and MC2 are written by the power program and send data corresponding to the codes to the comparison unit. A DC - decoder is needed to check the correct operation of two MC1 and MC2. IM - indexing module is used to turn on the light indicators depending on the presence of the code in the decoder, for example,

it turns on the “RY- Red and Yellow” indicator for the “RY” code, and the “B” indicator if the code is not received. CB - comparison unit compares the data coming from MC1 and MC2 , and after comparing the data coming from MC1 and MC2, it switches to proximity switches in accordance with the incoming pulses, and this code opens and closes them proportionally. CSU - contactless switch unit is oriented to open and close pulses and intervals according to these codes based on the information coming from the supply unit[18].

Development of a circuit for a microelectronic code transmitter

Microelectronic code transmitter based on the above functional diagram a circuit diagram was developed and its operation was verified using the Proteus program (fig. 2.)

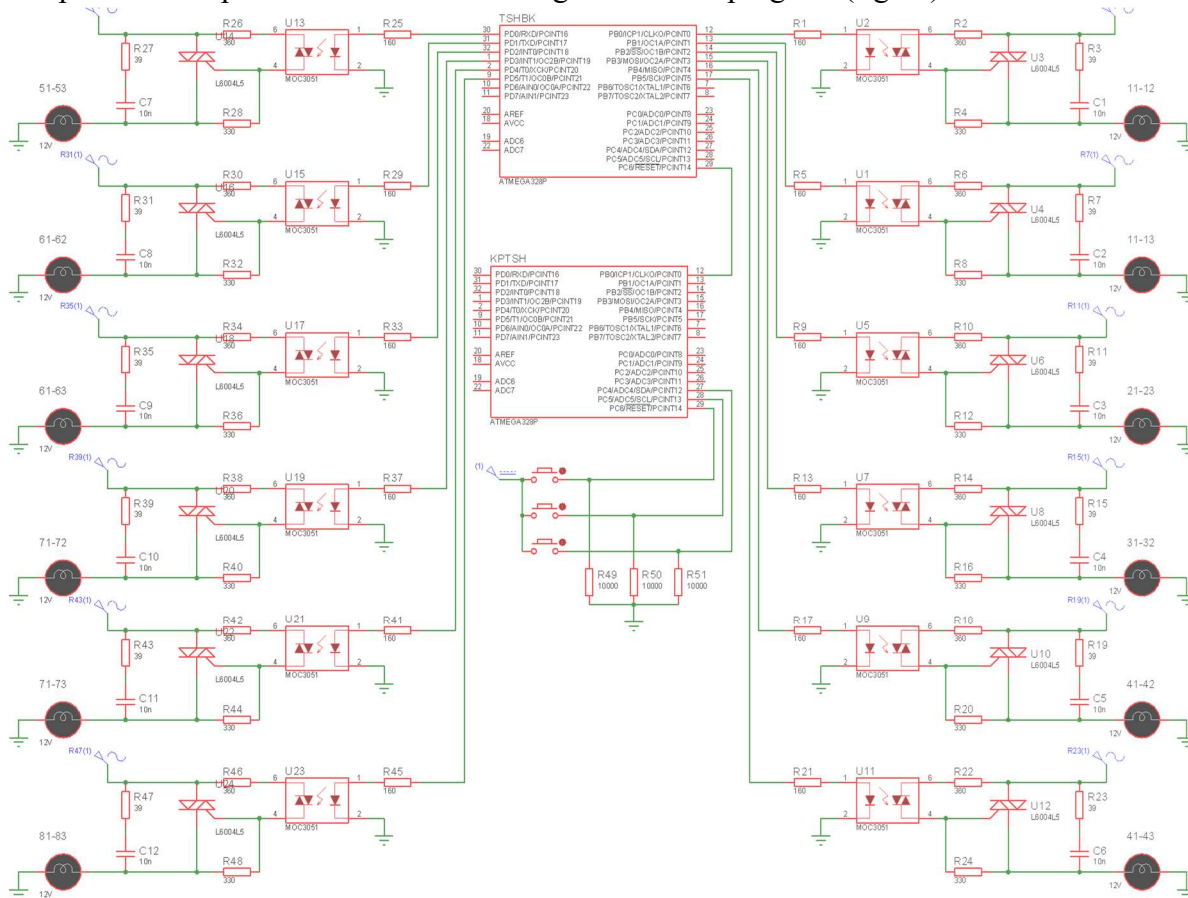


Figure 2 Diagram of a microelectronic code transmitter in the Proteus program.

In the Proteus program, the IMCT circuit diagram included the following several functional parts: 1. Microprocessor unit. 2. Indication circuit 3. Consists of KPTSH for checking the operation of proximity switches and TSH.

Proximity switches consist of optocouplers and triacs and have control and controlled signals, these two signals are provided by galvanic isolation.

Optocouplers are used as an element that performs the function of galvanic isolation. The voltage required to operate this device is simultaneously applied to the LED in the optocoupler.

Their burning is carried out by a photodiode, which serves to generate current. As a result, the circuit designed to control the switched-on device is activated

In addition, when developing a device, it allows the use of special optoelectronic devices, such as an opto- and photoresistor [12–16].

The device includes proximity switches 11-12, 11-13, 21-23, 31-32, 41-42, 41-43, 51-53, 61-62, 61-63, 71-72, 71-73 and 81-83 installed.

The basis of the microprocessor unit is the ATMEGA328P class microcontroller. The microcontroller performs the task of receiving pulses and codes generated in the KPTSH road code sensor and transmitting them to proximity switches[17].

To check the operation of the microelectronic code transmitter through the Proteus program, a code generator (KPTSH) is additionally installed. The KPTSH device is equipped with 3 separate buttons "RY -for Red and Yellow", "Y -for Yellow" and "G- for green" each code.

If the "RY" button is pressed, a voltage appears in block 27 of the KPTSH device, the RS6 input is activated, and the device develops the RY code, and through the RV0 output, pulses in the form of the RY code arrive from the 12-29 network to the RS6 input of the IMCT device. In the normal state of the IMCT, there was a logical 1 (5V voltage) from the outputs PB1, PB2, PB5, PD0, PD2, PD4 and PD5. When the pulse arrives, the microelectronic device supplies its outputs RV0, RV3, RV4 and RD1. As a result, it passes through the limiting resistors R1, R13, R17 and R29 of the device and comes to the optocoupler.

The term "Control" is used for the signal to the optocoupler, because the control signal (5 V) from the microcontroller turns on the photodiode and opens the triac inside the optocoupler.

Now the controlled signal passes through the limiting resistors R2, R14, R18 and R30 and comes to the controlled element of the triac through the open optocoupler. As a result, the circuit breaker opens and switches 11-12, 31-32, 41-42 and 61-62. According to the time diagram "RY" (Fig. 3), contactless switches 11-12, 31-32, 41-42 and 61-62 remain connected for 230 MS for continuous pulse delivery.

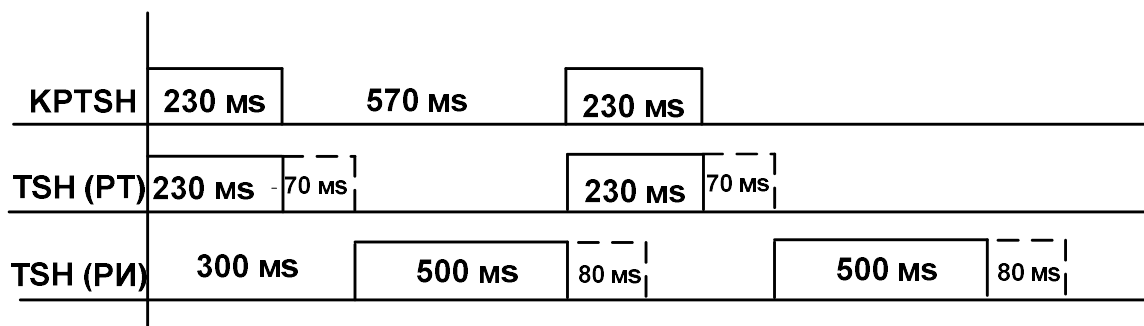


Figure 3. Diagram of temporal characteristics of impulses and intervals in the code "RY" for relay-transmitters TSh-65 and TSh-2000

After the 230MS timer has expired, the 70ms delay time will start to open proximity switches 11-12, 31-32, 41-42 and 61-62. After these delay times, the microelectronic code transmitter at the output of PD3 has a voltage of 5 V. Through block 2, it passes through the limiting resistors R37 and enters the optocoupler. The control signal to the optocoupler turns on the photodiode and the triac

inside the optocoupler opens. And the controlled signal passes through the limiting resistor R37 and enters the triac control element through an open optocoupler, and the triac opens and closes proximity switches 71-73, this connection lasts 570 MS. After a delay of 80 MS, the 2nd pulse starts to flow and the proximity switches 11-12, 31-32, 41-42 and 61-62 are connected in the above order. Disabling these proximity switches will enable proximity switches 71-72. Switches 71-73 remain on for 570 MS, and after 570 MS the switches turn off.

Thus, the first cycle ends and the second cycle begins before the 80MS interval end delay expires, and the microcontroller starts the above processes again. A light is on on the display unit, indicating the arrival of the code"RY". This process continues until the code is exchanged in the rail circuits (until another button is pressed on the KPTSH device).

The principle of operation of the device is the same for all codes, but they differ from each other in the number and duration of pulses and intervals. Instead of the "RY" light bulb, the "Y" or "G" light bulbs on the display unit light up.

During the initial check, the clock generator, the timer, the enable and reset circuits of the indication, and the service program return to the following modes[17-19]:

Initial setup steps:

- set the type of microcontroller;
- security bit off, WDT off;
- standard XT - generator.
- determination of the state of special-purpose registers;
- configure port B for output;
- configure port D for output;
- configure port C for access;
- determination of the state of special-purpose registers;
- Setting registers 1, 2 and 3 as a half cycle timer;
- Check PC6 for 1;
- if 0, set outputs PB1, PB2, PB5, PD0, PD2, PD3, PD4, PD5 to 1;
- if 1 setting outputs RV0, RV3, RV4 and RD1 to 1;
- return to the beginning of the program;

The program then loops and stays that way until an interrupt occurs to change the signal potential of the port.

Discussion.

Above is shown the software operation algorithm when using the integrated microelectronic code transmitter device based on the Proteus software. In this algorithm, a pulse and an interval are specified, so the normal state of the ports is the same for all encoders. The operating time of the ports and the number of pulses and code matching intervals change only in proportion to the incoming code.

For example, for the code «RY» there is one pulse and one interval, and for the code "Y" - two pulses and two intervals. In the software, all inputs and outputs work in the same order for the codes “RY”, “Y”, and “G”, but the pulse duration and intervals are different.

References

1. Soroko V. I., Fotkina Zh. V. Equipment for railway automatics and telemechanics: Reference book: in 4 books. Book. 1. - 4th ed. - M.: LLC "NPF" PLANET", 2013 - 1060 p.
2. Kazanov A. A. et al. Systems of interval regulation of train traffic / A. A. Kazakov, V. D. Bubnov, E. A. Kazakov: A textbook for railway technical schools. transp. — M.: Transport, 1986. — 399 p.
3. Kazakov A.A., Bubnov V.D., Kazakov E.A. Automated systems for interval control of train traffic: Textbook, for technical schools of the railway. transp. M.: Transport, 1995. - 320 p.
4. Theeg G., and Vlasenko S. "Railway Signaling & Interlocking - International Compendium", Eurailpress, 2009, 448 p.
5. Saitov, A., Kurbanov, J., Toshboyev, Z., & Boltayev, S. (2021). Improvement of control devices for road sections of railway automation and telemechanics. E3S Web of Conferences, 264, 05031. doi:10.1051/e3sconf/202126405031.
6. Sapozhnikov V., Sapozhnikov V., Efanov D. and Nikitin D., "Combinational circuits checking on the base of sum codes with one weighted data bit," Proceedings of IEEE East-West Design & Test Symposium (EWDTS 2014), 2014, pp. 1-9, doi: 10.1109/EWDTS.2014.7027064.
7. Table of content. (2015) (pp. 1–9). Institute of Electrical and Electronics Engineers (IEEE).<https://doi.org/10.1109/dynamics.2014.7005631>
8. Liudvinavičius, L., Dailydka, S., & Sładkowski, A. (2016). New possibilities of railway traffic control systems. Transport Problems, 11(2), 133–142.<https://doi.org/10.20858/tp.2016.11.2.13>
9. Havryliuk, V. (2020). Detecting of Signal Distortions in Cab Signaling System Using ANFIS and WPESE. In 2020 IEEE 4th International Conference on Intelligent Energy and Power Systems, IEPS 2020 - Proceedings (pp. 231–236). Institute of Electrical and Electronics Engineers Inc.<https://doi.org/10.1109/IEPS51250.2020.9263165>
10. Havryliuk, V.O. (2018). Modeling of the Return Traction Current Harmonics Distribution in Rails for AC Electric Railway System. In IEEE International Symposium on Electromagnetic Compatibility (Vol. 2018-August, pp. 251–254). Institute of Electrical and Electronics Engineers Inc.<https://doi.org/10.1109/EMCEurope.2018.8485160>
11. Tandon, S., Subramanian, K., Moundekar, T., & Khanna, V. (2018). Improvement in speed of trains in poor visibility & advancement of train transport signaling mechanism. International Journal of Engineering and Technology(UAE), 7(2), 221–227.<https://doi.org/10.14419/ijet.v7i2.23.11923>
12. D. Nikitin, A. Nikitin, A. Manakov, P. Popov and A. Kotenko, "Automatic locomotive signalization system modification with weight-based sum codes," 2017 IEEE East-West Design &

Test Symposium (EWDTS), 2017, pp . 1-5, doi: 10.1109/EWDTS.2017.8110099.

13. Bose, B., & Lin, DJ (1985). Systematic Unidirectional Error-Detecting Codes. IEEE Transactions on Computers, C-34(11), 1026-1032. <https://doi.org/10.1109/TC.1985.1676535>

14. Fujiwara, E. (2005). Code Design for Dependable Systems: Theory and Practical Applications. Code Design for Dependable Systems: Theory and Practical Applications (pp. 1–701). John Wiley and Sons. <https://doi.org/10.1002/0471792748>

15. Hololobova, O., Buriak, S., Havryliuk, V., Skovron, I., & Nazarov, O. (2019). Mathematical modeling of the communication channel between the rail circuit and the inputs devices of automatic locomotive signalization. MATEC Web of Conferences, 294, 03009. <https://doi.org/10.1051/mateconf/201929403009>

16. Kovkin, A.N. Methods for constructing non-contact devices for interfacing a control computer complex with executive objects of railway automation systems: dissertation ... candidate of technical sciences: 05.22.08 / Kovkin, Alexey Nikolaevich; [Place of protection: Petersburg. state University of Communications]. - St. Petersburg, 2005. - 188 p.

17. Turanov K, Gordienko A, Saidivaliev S, Djabborov S (2020) Designing the height of the first profile of the marshalling hump. E3S Web of Conferences 164:03038. <https://doi.org/10.1051/e3sconf/202016403038>

18. Turanov K, Gordienko A, Saidivaliev S, Djabborov S (2020) Movement of the wagon on the marshalling hump under the impact of air environment and tailwind. E3S Web of Conferences 164:03041. <https://doi.org/10.1051/e3sconf/202016403041>

19. Turanov K, Gordienko A, Saidivaliev S, Djabborov S, Djalilov K (2021) Kinematic Characteristics of the Car Movement from the Top to the Calculation Point of the Marshalling Hump. In: Murgul V, Pukhkal V (eds) International Scientific Conference Energy Management of Municipal Facilities and Sustainable Energy Technologies EMMFT 2019. EMMFT 2019. Advances in Intelligent Systems and Computing 1258. <https://doi.org/10.1007/978-3-030-57450-529>